

## Chapter 1

### Introduction

In this work, we will explore how light travels through highly scattering media. Although we are primarily concerned with light diffusion through tissue for medical diagnostic purposes, there are many applications of interest. For example, clouds, paint and foams are all highly scattering media. We model the transport of light through the media as a diffusion process. The analysis used here can be applied to other diffusional processes such as heat diffusion, neutron diffusion, or chemical diffusion.

In this chapter we will briefly review some uses of light in medical diagnostics. Next we will give an overview of diffuse photon imaging. As in most imaging techniques, creation of an image requires an understanding of the interaction between the probe and the media (i.e. the forward model). The forward model relates a measurement to the optical properties of the medium. When the forward problem is well understood, a series of measurements are made, and finally, the measurements and the forward model are used together to derive a map of the properties of the medium (i.e. the inverse problem). We will outline some popular forward models and inversion methods, and discuss the resolution of diffusive wave based optical imaging and the types of contrasts measurable using optical probes.

## 1.1 Historical Perspective

As early as 1929, researchers investigated passing bright light through the body to create shadow images [1]. These transillumination images were of poor quality because light is multiply scattered as it passes through tissue, and it is difficult to separate scattering effects from absorption effects. In the past 20 years, a better understanding of how photons travel through tissue has enabled researchers to correlate internal physiological changes to optical changes. We and other investigators have begun to image these optical changes using a variety of methods.

As the diagnostic power of optical measurements is improved, optical measurements are expected to gain wider acceptance within the medical community. Recent technological developments afford the possibility of compact, low cost medical optical instruments. In low power (less than 100 mW peak power) near infra-red studies, the developments include light emitting diodes and laser diodes, which replace table top laser systems used in research laboratories, and solid state detectors such as the avalanche photodiode which have a fast response time and broad spectral sensitivity.

Most medical optical instruments use single scattering to probe tissue at or near its surface. Laser Doppler flow-meters and angiograms are examples of near surface measurements. In this work we are interested in developing instruments which probe more deeply (3 - 10 cm) into the tissue.

An example of an instrument which uses multiply scattered light is the finger pulse meter. Here the amount of light which passes through a patient's finger changes as blood pressure causes vessels to expand and contract. As the finger fills with blood and expands, the amount of transmitted light decreases. This change in transmission is currently used to continuously, and non-invasively monitor the pulse rate of many intensive care patients.

An improvement to the pulse meter introduces the use of spectral filters to compare light transmission at different wavelengths. If we examine the water absorption spectra of the major tissue chromophores (figure 1.1), we see that in the near infra-

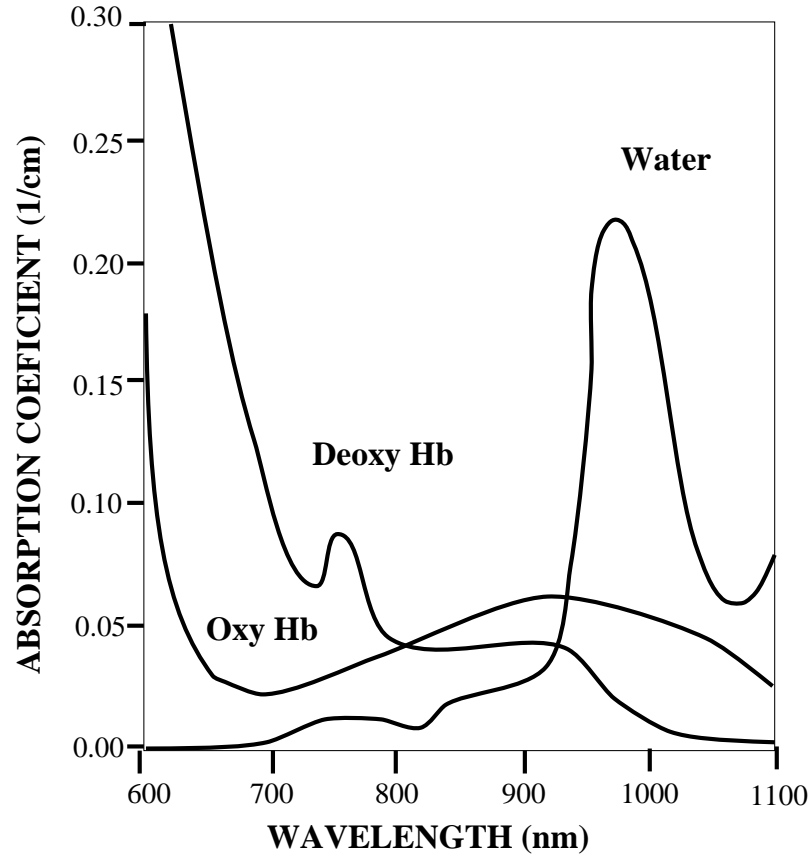


Figure 1.1: Absorption spectra of major skin chromophores. Courtesy of K.S. Reddy, University of Pennsylvania.

red, the absorption is low, and there is a crossover point between oxygenated and de-oxygenated hemoglobin. In simple devices such as the RunMan<sup>TM</sup> [2] shown in figure 1.2, two wavelengths are used to measure qualitative trends in blood oxygenation (see figure 1.3). The optical probe consists of a pair of small tungsten light bulbs which give brief flashes of light every second (The peak power is less than 1 W, the average power is less than 0.5W.) The white light migrates through the tissue and is collected by silicon diode detectors at wavelengths selected by gelatin optical filters at the surface of the detector. Typically one detector uses a 760 nm filter, and the other a 850 nm filter. It is assumed that the blood is the prominent absorber at these wavelengths, so the absorption at 760 nm is predominately from de-oxygenated hemoglobin

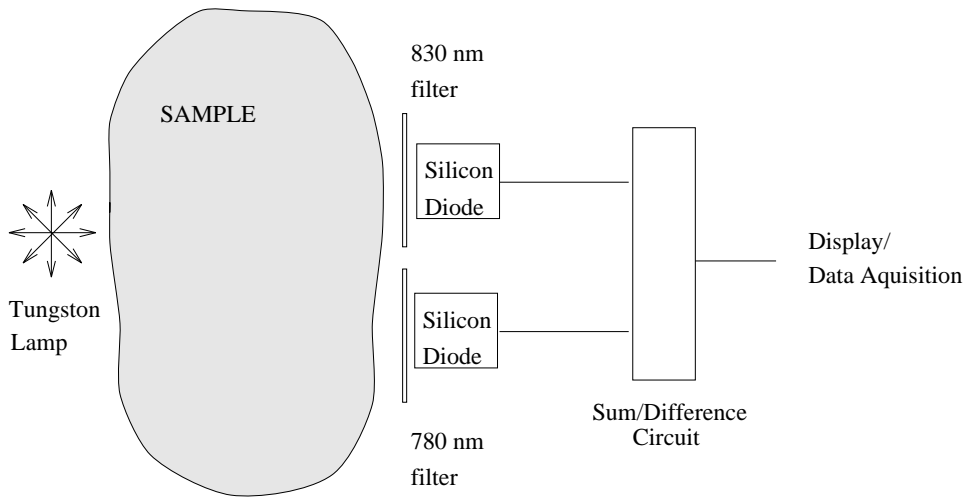


Figure 1.2: A simplified schematic of the RunMan<sup>TM</sup> instrument.

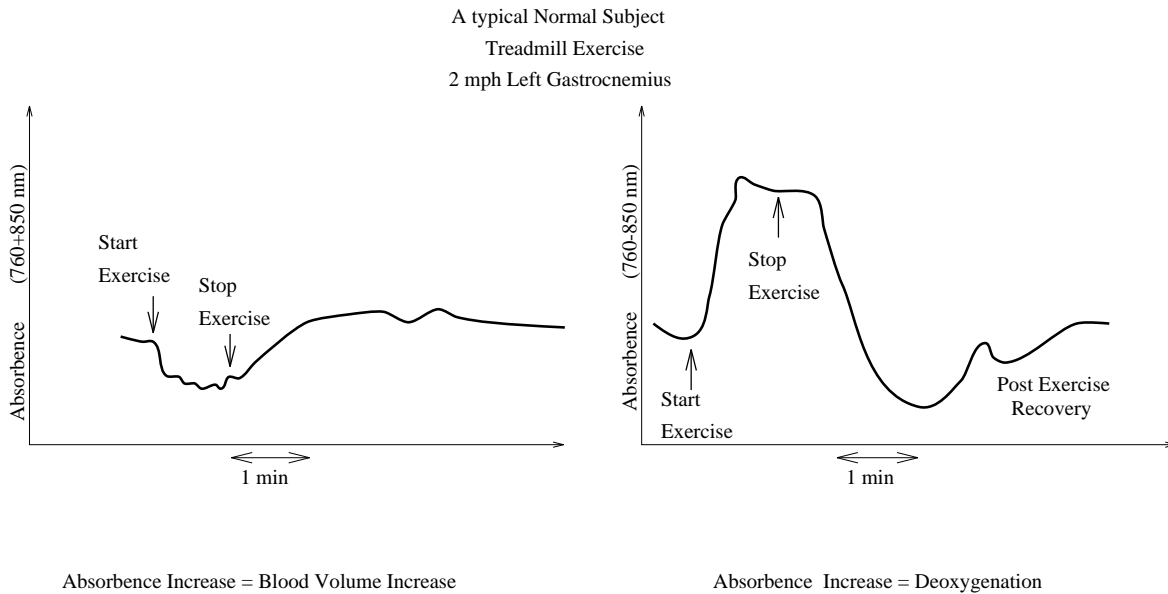


Figure 1.3: A typical RunMan<sup>TM</sup> oxygenation trace. Courtesy of B. Chance, University of Pennsylvania. Note that as the exercise begins, the muscle contracts and the blood volume decreases. This results in a decreased absorbance in both 760 nm and 850 nm light. At the same time, the muscle begins to use oxygen resulting in a decrease in oxygenated blood concentration (850 nm) and an increase in de-oxygenated blood concentration.

and the absorption at 850 nm is predominately from oxygenated hemoglobin. The sum of the two signals is an indicator of blood volume changes, and the difference is an indicator of a change in oxygenation. These qualitative trends are used in exercise studies for professional athletes, analysis of myoglobin disorders, and the detection of hematomas.

## 1.2 Photon Diffusion Equation

In 1988 Patterson *et al.* [3] experimentally demonstrated that the propagation of light through tissue is well described by a diffusion equation. Thus analogies between light transport in tissues and the theories of heat diffusion and neutron diffusion were possible. This idea allowed researchers to quantify the average absorption and scattering of a region of tissue by fitting the diffusion solution to their measurements. These early experiments were performed with a pulsed laser source and a time resolved measurement of the response. Researchers quickly realized that similar experiments could be done in the frequency domain using amplitude modulated light sources, and measuring the amplitude and phase of the diffusing photon density waves [4]. For amplitude modulated sources in homogeneous media, the diffusion equation for the oscillating part of the light energy density reduces to a Helmholtz equation with simple spherical wave solutions. Microscopically, the waves are composed of random walking photons with a random walk step on the order of 1 mm, but macroscopically, the photons add to form a damped, scalar wave of photon density with a wavelength on the order of 10 cm in biological tissue. We will refer to this wave as the diffuse photon density wave (DPDW).

The wave analysis allows us to draw analogies from the field of electromagnetic radiation, providing valuable insight, as well as computational ease. These waves have been shown to diffract around an edge [5], refract and obey Snell's Law [6], diffract or scatter from localized heterogeneities [7], and exhibit well defined dispersion characteristics [8]. The properties of DPDW's have been verified in both biological models [5] and human breast studies [9]. We have shown that DPDW's scatter from large

spherical inhomogeneities in a way that is similar to, but simpler than, Mie scattering [10]; and that DPDW's in a fluorescent medium are absorbed and then re-radiated creating fluorescent DPDW's whose wavelengths are governed by the optical properties of the medium at the Stoke-shifted optical wavelength [7, 11, 12].

### **1.3 Introduction to Optical Imaging**

Since the advent of the photon diffusion equation, researchers have struggled to accurately measure the optical properties of biological systems. For example, the head is made up of blood, white matter, grey matter, bone, skin, etc. Each of these types of tissues has different optical properties. If one assumes a homogeneous model to calculate the average optical properties, one cannot obtain accurate values for the absorption and the scattering. Instead, an average value of the tissue optical properties is derived. Thus, there has been a great deal of interest in creating a quantitative map or "image" of the optical properties. In particular, physicians are interested in functional imaging and the localization and characterization of tumors and hematomas.

A sample optical image is shown in figure 1.4. The sources and detector are scanned around the region of interest as shown in (a), and the measurements are used to reconstruct a map of the absorption.

The methods and algorithms one uses to image with diffuse photons are similar in many ways to x-ray tomography. A source and detector are scanned around the surface of the tissue volume of interest, and the measurements are inverted to reconstruct the optical properties within the tissue volume as a function of position. Although most of the images created to date are of tissue phantoms, preliminary images have been generated of breast [13] and neonatal brain [14].

#### **1.3.1 Forward Models**

Nearly all imaging algorithms can be divided into two stages. First, an algorithm must have a model of the forward problem. The forward model describes the passage of photons through the heterogeneous medium. For the image reconstruction, the

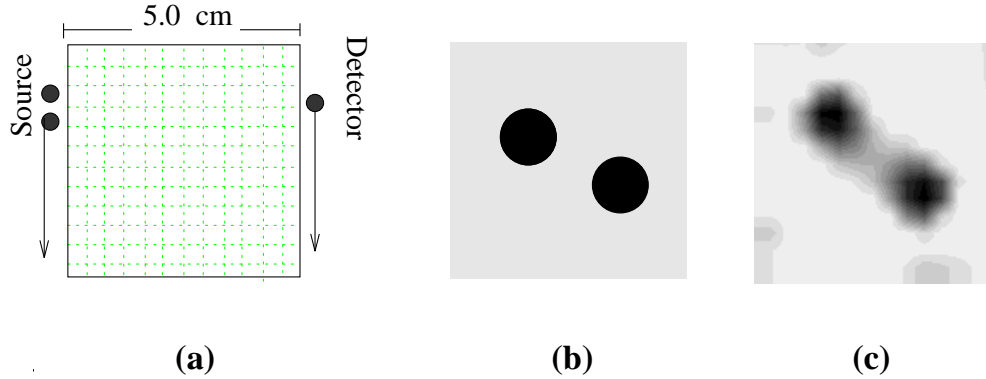


Figure 1.4: A reconstruction of two absorbing objects. (a) The scanning geometry. The sources and detector scan around the edges of a 5 x 5 x 1 cm region while two absorbing spheres are hidden in the region (b). (c) The reconstructed absorption map. (Born approximation, 3000 SIRT iterations)

region of interest is divided into a set of volume elements (voxels). Generally, the forward algorithm provides a weight (or importance) to each voxel within the sample volume, and the measured signal is a function of these weights. One can think of the the weights as being proportional to the probability of photons from a source reaching a particular voxel, and then continuing on to reach the detector position. We will derive precise definitions of the weights in chapter 4.

In x-ray tomography, it is assumed that the intensity signal decays exponentially as it passes in a straight line from source to detector. In this case the log of the measured intensity ( $I$ ) divided by the initial intensity ( $I_o$ ) is

$$\ln(I/I_o) = -\int_0^L \alpha(l)dl \quad (1.1)$$

where  $L$  is the source-detector separation, and  $\alpha(l)$  is the absorption coefficient as a function of position,  $l$  along the line connecting the source and detector. The unknowns are the position dependent x-ray absorption coefficients. This equation may be digitized into  $N$  pieces of length  $h$ ,

$$\ln(I/I_o) = -\sum_{j=0}^N \alpha_j h \quad (1.2)$$

$$measurement = \sum unknown \times weight. \quad (1.3)$$

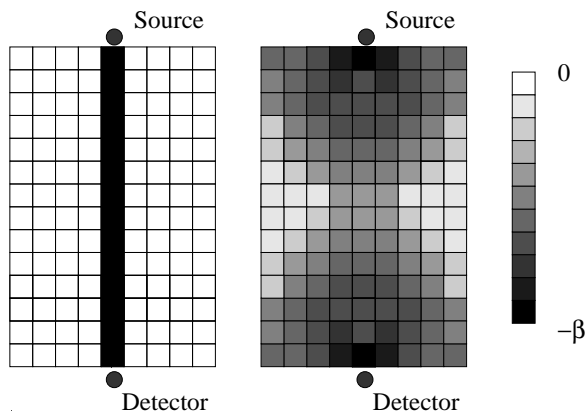


Figure 1.5: Sample weight distributions for CAT (left) and diffuse photon imaging (right).

Now we have a relation between the transmission measurement and the unknown,  $\alpha_j$ . The relation is a function of a calculable quantity called the weight. In this case the weights along the line are all  $-\beta$ .

Traditional imaging techniques such as x-ray tomography typically give equal, non-zero weights along the source-detector line of sight, and zero weights elsewhere. This is a good approximation because detected x-rays do not scatter very much as they move through the tissue, so detected x-rays rarely sample tissue outside of this line. In diffuse photon imaging, the diffusive waves emanate spherically outward from a source, and thus sample tissue well outside the straight line of sight. The weights are usually non-zero over most of the region of interest as shown in figure 1.5.

In our lab, we developed a forward model which is an approximate solution to the heterogeneous diffusion equation. (In particular we use either a Born or Rytov approximation.) These solutions give us explicit forms for the weights which are functions of the properties of the medium, the modulation frequency, and the position of the source and detector.

Other investigators have chosen to use empirical weights based on measurements made in model systems. For example, investigators have placed a small point-like absorbing object in an otherwise homogeneous medium and determined its effect on the measured signal [15]. By moving this object to each voxel, one can generate a set



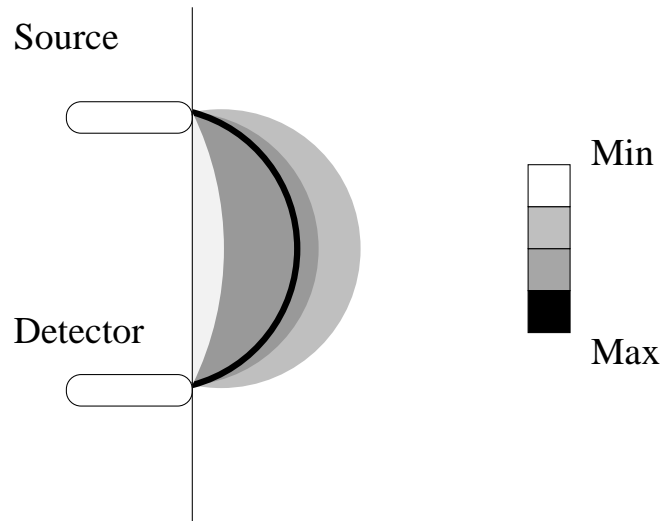


Figure 1.6: Sample weight distributions for a pulsed source on the surface of a semi-infinite medium.

of weights for a particular source detector geometry. These weights have been verified in simple geometries using a three point Green function approach [15]. Studies such as these have shown that the weights in a semi-infinite medium may be roughly described by the so called “banana function” (see figure 1.6). Nioka *et al.* have developed a model in which the weights are generated by hand based on this banana pattern [2].

A numerical solution to the heterogeneous diffusion equation using finite difference, finite element or Monte Carlo simulation are other robust but time consuming methods of generating the weights. The advantage of these calculations is that they can accurately model irregular boundary conditions and heterogeneous media. The analytic solution for a homogeneous system with an embedded spherical or cylindrical object can also be used to generate the weights. As a rule, the more approximate models such as the straight line approximation, and the empirical functions are quick to calculate. The most precise models such as the finite difference and Monte Carlo can take days to calculate. Table 1.1 lists some of the popular forward models with a rough estimate of the calculation time for each.

<b>Model</b>	<b>Typical CPU time</b>	<b>References</b>
Approximate solution to diffusion equation	seconds	[16],[17],[18],[19]
Empirical solution	seconds	[14],[2],[15]
Straight line (x-ray) model	seconds	[13]
Finite Difference/Finite Element	hours	[20],[21]
Monte Carlo	days	
Analytic Solutions	minutes	[22]

Table 1.1: Popular forward models for photon diffusion imaging. These times are rough estimates for a system with about 100 source-detector pairs and 500 voxels covering a 6 cm x 6cm x 2 cm area.

### 1.3.2 The Inverse Problem

The object of tomographic imaging is to use some set of measurements to solve for the properties of the medium. We will see in chapter 4 that for forward model may be written in the following form;

$$measurement = \int_V weight \times unknown. \quad (1.4)$$

Using Fourier transform methods, it may be possible to invert this integral equation to solve for the unknowns. These methods are currently under investigation in our laboratory and in other laboratories [23, 24]. This equation can be approximated as a discrete matrix equation;

$$measurement_i = \sum_j weight_{ij} \times unknown_j. \quad (1.5)$$

Where  $i$  enumerates the measurements, and  $j$  enumerates the voxels. After specifying the forward model which describes the passage of photons through heterogeneous

media, the investigator must then invert the problem to solve for the unknown optical properties in each voxel.

Table 1.2 lists some of the popular inversion methods. One set of methods is to directly invert the forward equations to solve for the unknowns. Theoretically, the direct matrix inversion should yield the unknowns in equation 1.5. But the inversion of a large matrix is a time consuming calculation, and due to the nature of the problem, the solutions are not unique. We will use regularization techniques to control the uniqueness problem. In addition, the inverse matrix can be pre-calculated and stored before the experiment.

There are many error minimization routines which find the unknowns by fitting the forward model to the measured data. The error minimization routines mainly differ in the way that they move from an initial guess toward the correct solution. Some error minimization methods, such as the algebraic reconstruction techniques (ART), are only valid for linear equations. In our lab we use both ART and a direct matrix inversion to create images. The relative merits of these techniques are discussed in chapter 4.

Back-projection algorithms, often used in creating x-ray images, are gaining popularity in photon imaging, especially for two dimensional projection images. Generally, a back-projection algorithm will give a fast, rough image. In some cases we have used a modified back projection method which is briefly described in appendix D.

## 1.4 Resolution

The resolution of images with diffuse photons is ultimately limited by the underlying length scale of the diffusion theory, the random walk step of the photon (typically about 1 mm in tissue). In our experiments, we have resolved two 1.2 cm diameter spheres separated by a center-to-center distance of 2 cm. The resolution is dependent on the wavelength of the DPDW. The shorter the wavelength, the better the resolution. However, the positive effect of shortening the wavelength is offset by the fact that the amplitude of the wave decays exponentially at a spatial rate inversely

<b>Method</b>	<b>Typical CPU Time</b>	<b>References</b>
<u>Direct Inversion</u>		
matrix inversion	hours	[19],[25],[18]
Fourier transform	seconds	[23],[26],[24]
<u>Error Minimization</u>		
algebraic reconstruction - ART	minutes	[17],[18],[19]
conjugate gradient	minutes	[17]
projection onto convex sets - POCS	minutes	[17]
least squares fitting	minutes	[20],[22]
<u>Back-Projection</u>	seconds	[15],[14],[2]

Table 1.2: Popular inverse models for photon diffusion imaging. These times are rough estimates for a system with about 100 source-detector pairs and 500 voxels covering a 6 cm x 6 cm x 2 cm area.

proportional to the wavelength ( $e^{kr}$ ). The shorter the wavelength, the smaller the measured signal. The wavelength can be shortened by increasing the modulation frequency or increasing the background absorption or scattering.

Boas *et al.* have used a noise analysis to study the limits of object detection and characterization [22]. The authors found that using a simulation based on realistic positional uncertainties and shot noise, objects whose optical properties are approximately twice the background levels and are 3 mm or larger can be detected and localized; and objects 5 mm or larger can be characterized. The authors studied a system designed to model a lightly compressed breast with an embedded tumor [27].

## 1.5 Contrast

Optical imaging provides fundamentally different information than MRI, x-ray or ultrasound imaging. Although we generate low resolution images, the contrasts are *optical* properties, and this opens the door to a host of new physiologic mechanisms. In our lab we have imaged absorption [28], the mean photon scattering length [18] (reduced scattering coefficient) and fluorophore lifetime and concentration [12]. In this thesis, we will concentrate on these studies. Other work in our lab has demonstrated imaging of the dynamic properties of scatterers, such as Brownian motion and flow in model systems [29].

It important to note that by varying the incident optical wavelength it becomes possible to perform spectroscopy in each of these contrasts. Researchers are just beginning to investigate and quantify the optical changes which accompany physiological changes in the body. There is considerable evidence that mitochondria are the dominant light scatterers in most tissues [30]. This corroborates studies which show that a rapidly growing tumor, which has an increased concentration of mitochondria, is generally more highly scattering than the surrounding tissue [31]. A tumor also has an increased vascularity, and thus a higher absorption due to the high volume fraction of blood [31].

In the past two years, there has been a great deal of interest in the non-invasive

detection of glucose changes in the body [32, 15]. Since scattering depends on a mismatch in the index of refraction, the presence of solutes such as glucose or potassium, which change the index of refraction of the intra- or extra-cellular fluid change the scattering properties of the system.

In addition to natural optical changes, a wide range of optical dyes have been developed for medical purposes. For example, the lifetime of some fluorescent dyes has been shown to vary with the amount of oxygen in its environment [33]. Some dyes have already been approved by the FDA for other uses, but happen to be quite useful for near infra-red imaging. Indocyanine green (ICG) has been used in liver studies for over 20 years. Usually the dye is injected into the blood stream, and small volumes of blood are taken every minute. The rapid decrease of ICG in the blood indicates a that a healthy liver is removing the ICG.

It is possible that ICG will prove to be a useful contrast agent for optical tumor detection. ICG has a strong absorption peak in the near infra-red (at 780 nm), and fluoresces at 830 nm making it an excellent candidate for optical studies. ICG's molecular size is roughly the same as gadolinium chelate. Gadolinium chelate has been shown to leak from the blood vessels in a rapidly growing tumor, and is currently used as a MRI contrast agent for tumor detection.

The remainder of this thesis will follow the outline below. After a discussion of diffuse photon density waves (chapter 2), the experimental apparatus we use to measure the amplitude and phase of the waves will be discussed (chapter 3). Then we move on to imaging. In chapter 4 we discuss the forward model and inverse algorithms used to image inhomogeneous absorption. Computer simulated experiment and experimental results are shown. Next we describe a parallel analysis for inhomogeneous scattering (chapter 5). Finally, we examine systems with both absorption and scattering changes (chapter 6). In chapter 7 we discuss diffuse photons in a fluorescent media. We develop the theory which describes fluorescent diffuse photon density waves, show how these fluorescent waves can be used to locate the center of a fluorescent object, and finally we show that the lifetime and concentration of fluo-

rophore can be tomographically imaged in a manner similar to the absorption case. Additional background information on singular matrices, time resolved spectroscopy and the time-domain fluorescent DPDW derivation is given in appendices A , B, and C respectively. The results of some preliminary back-projection imaging work are shown in appendix D. Appendix E gives an overview of the PMI software program developed in our lab, and appendix F demonstrates a increase in PMI processing speed using parallel processing.

